https://doi.org/10.3311/PPci.41050

Periodica Polytechnica Civil Engineering, 69(3), pp. 991–998, 2025

Response Spectrum of Piecewise Linear Elastic Structures

Róbert K. Németh[1*], Abdalla M. K. Elhadi[1]

[1] Department of Structural Mechanics, Faculty of Civil Engineering, Budapest University of Technology and Economics, Műegyetem rkp. 3., H-1111 Budapest, Hungary
[*] Corresponding author, e-mail: nemeth.robert@emk.bme.hu

Received: 17 May 2025, Accepted: 24 July 2025, Published online: 30 July 2025

Abstract

Response spectra are helpful in the structural engineering practice for the design with earthquake as an extreme load case. However, it is restricted to the linear analysis, except for the plastic behavior. The linear analysis uses a single stiffness only, and by this, the low-level nonlinearities, as the opening and closure of cracks in reinforced concrete structures, are neglected. In this paper, we investigate single-degree-of-freedom systems with two linear elastic states. The response of the piecewise linear elastic structure is compared to the linear response for artificial earthquake accelerograms confined to a design response spectrum. The analysis shows that a high difference in the stiffnesses of the two states may result in a considerable increase in the response. At the same time, states with small relative differences in their stiffness have a maximum response below or close to the response of the linear system. Thus, the neglect of the low-level nonlinearity, as the opening and closing of a crack does not affect the assessment of the structure.

Keywords

earthquake analysis, piecewise linear elastic structure, response spectrum

1 Introduction

Earthquakes have a significant role in the design of engineering structures. While classic load cases are dominantly static, the earthquake is, by its origin, a dynamic effect. Structurally, the earthquake acts as a support vibration, and the dynamic response of the structure is in the primary scope of the analysis. Building codes [1, 2] offer response spectra, where the maximum relative displacements with respect to the supports (the deformations) can be obtained as a function of the structure's natural period. For instance, the European code specifies parameters to select the appropriate response spectrum based on the region and damping level and many other factors [1]. However, it does impose restrictions on the use of these spectra for linear analysis. The only nonlinearity is related to the plastic deformations: the hysteretic nature of the material property can be included in the behavioral coefficient. We note here that the application of the response spectrum requires the evaluation of the fundamental or the relevant natural periods of the structure. These periods are evaluated on the linear system.

As a general rule, the building codes allow the application of the design spectrum for linear problems. For nonlinear problems, the pushover analysis or an incremental dynamic analysis is required. However, the nonlinearity caused by the plastic deformations can be implemented in the analysis through the behavioral coefficient. This approximation is justified by many numerical and laboratory tests from the early days until the recent times, see, e.g. [3, 4]. A different form of material nonlinearity can be found in reinforced concrete structures: during vibration, the cracks may close and open again. That way, the working cross-section varies depending on the current configuration, resulting in a nonlinear stiffness. Opening and closing gaps can be found in masonry structures as well [5, 6], so the phenomena is not restricted to the RC-structures.

Assuming the closure of a single crack, we can distinguish between two, piecewise linear elastic states of the structure. Piecewise linear elastic structures are a special group of nonlinear structures where the current state of the structure affects the otherwise linear stiffness. Simple examples of these behaviors are the above mentioned opening of cracks, the closing of gaps, but the slackening of cables [7] and the rocking motion of structures [8] belongs here, too.

The linear response spectrum deals with one state only, leaving open the question whether the neglect of this nonlinearity is safe or not. While the connection of the response spectrum analysis and the pushover analysis

Cite this article as: Németh, R. K., Elhadi, A. M. K. "Response Spectrum of Piecewise Linear Elastic Structures", Periodica Polytechnica Civil Engineering, 69(3), pp. 991–998, 2025. https://doi.org/10.3311/PPci.41050

was investigated in [9], otherwise, to the current knowledge of the authors, the question of how the concept of the response spectrum can be generalized in view of the two states is still open.

So, in this paper, as an initial step, we will analyze the state-wise extremal displacement caused by an artificial forcing which has a response spectrum conforming to the design spectrum. The motivation behind this analysis is to characterize the possible error introduced by the piecewise linear elasticity and to identify its magnitude.

The structure of the paper is as follows. In Section 2, we review the meaning and application of the linear response spectrum, show the steps of the generation of the artificial time-history functions used in the analysis and the time-step analysis of the PL-elastic model. In Section 3, we introduce a definition of the PL-spectrum of a two-state structure and show an example of its calculation. In Section 4, we perform a thorough analysis with 20 generated time-histories and compare the results to those of the linear analysis, where one of the states would be neglected. In Section 5, we summarize our results and draw the conclusions.

2 Model and methodology description

2.1 Linear response spectrum

For a given $z(t)$ support motion, the differential equation of a single degree of freedom model can be written for the $u(t)$ relative displacements as

$$m\ddot{u}(t)+c\dot{u}(t)+ku(t)=-m\ddot{z}(t), \tag{1}$$

where m is the mass of the structure, c is the damping coefficient, k is the spring stiffness, and the dot represents differentiation with respect to time. To decrease the number of system parameters, the differential equation can be reformulated to

$$\ddot{u}(t)+2\xi\omega_0\dot{u}(t)+\omega_0^2u(t)=-\ddot{z}(t), \tag{2}$$

where $\xi=c\Big/\left(2\sqrt{km}\right)$ is the damping ratio and $\omega_0=\sqrt{k/m}$ is the natural circular frequency. The latter is indirectly proportional to the natural period, as $T_0=2\pi/\omega_0$.

The response spectrum of a fixed $z(t)$ support motion is taken from the solution of the Eq. (2) (the $u(t)$ response, in this paper calculated everywhere with the Newmark-method), as

$$S_u\left(T_0\right)=\max\left|u(t)\right|. \tag{3}$$

Here, the absolute value represents that the support motion could occur in the same direction, i.e. as $-z(t)$. For practical purposes, the pseudo-acceleration response spectrum can be introduced as

$$S_{PA}\left(T_0\right)=\omega_0^2S_u\left(T_0\right). \tag{4}$$

Using this, the $m\times S_{PA}(T_0)$ static force generates the same absolute valued displacements, deformations, internal forces, etc., as the maximum caused by the $z(t)$ support motion.

During a design process, the $z(t)$ support vibration is an unknown function. For these cases, building codes provide design response spectrum, where stochastically specified values of the Eq. (4) spectrum are given. Applying these spectrum values based on the natural period follows the same rules. The S_d design spectrum value must be evaluated as a function of the fundamental period, and the $m\times S_d$ force must be applied as a static force on the structure. Furthermore, the vibrating nature of the forcing requires a second load case as well, where the $-m\times S_d$ force must be applied.

2.2 Artificial time-history generation

Following the classic approach of [10], we create the artificial accelerogram functions in the form:

$$\ddot{z}(t)=\sum_{j=1}^{N}I(t)A_j\cos\left(\omega_jt+\varphi_j\right), \tag{5}$$

where

- $I(t)$ is an intensity function,
- N is the number of harmonic components of the generated function,
- ω_j-s are the circular frequencies of harmonic components of the generated function,
- φ_j-s are the phase angles of harmonic components of the generated function,
- A_j-s are the amplitudes of harmonic components of the generated function.

A recent comparison of other methods can be found in [11]. The generation of the $\ddot{z}(t)$ function means that for a fixed set of frequencies and intensity function, we take a random set of phase angles, and in an iterative process, we tune the amplitudes such that in the specified frequencies, the estimated response spectrum value fits the design value. Figs. 1 and 2 show the detailed steps of the above process as follows.

Fig. 1 (a) shows the target spectrum taken from the Eurocode [1]. We have chosen a type 1 curve with the following parameters. The lower and upper limits of the constant spectral acceleration branch are T_B = 0.2 s and

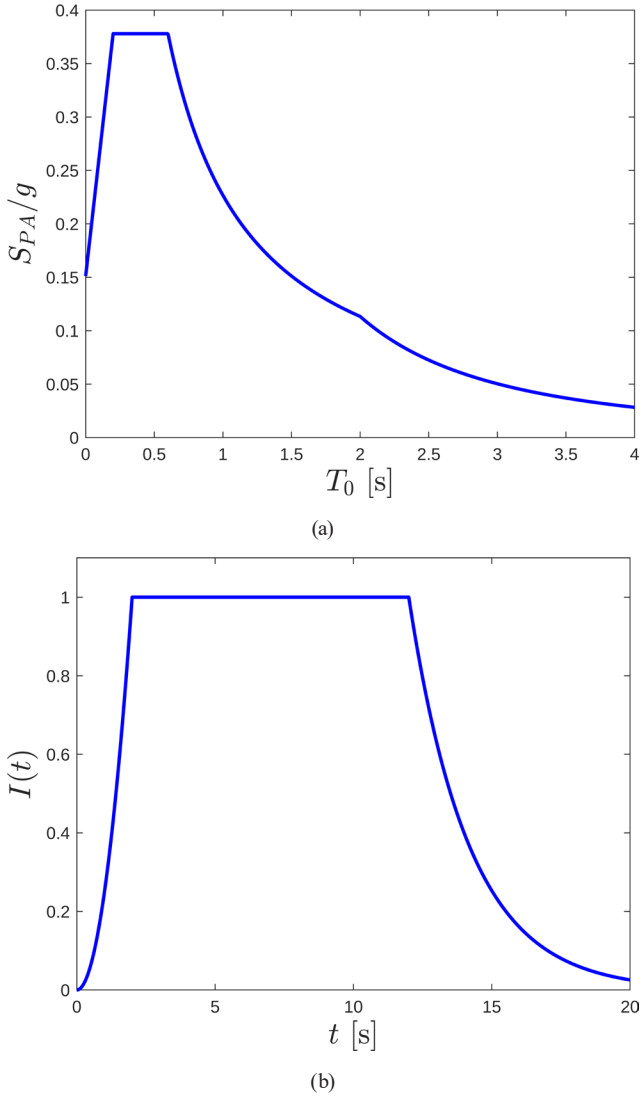

Fig. 1 (a) The target spectrum used for the generation of accelerograms, (b) The $I(t)$ intensity function used in the generation

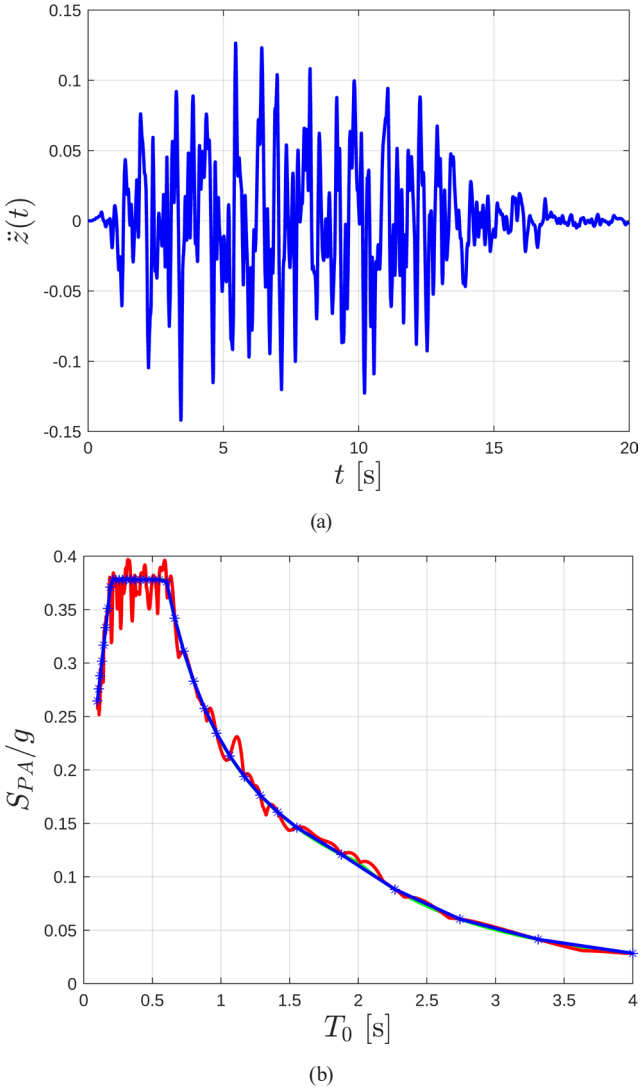

Fig. 2 (a) One example of the artificially generated accelerograms, (b) Response spectrum of the example function (green line is the target spectrum, blue line connects the points in the harmonics of the function, red line is the response spectrum of the generated $\ddot{z}(t)$ function)

$T_C = 0.6$ s, where the maximum spectral amplification factor is $\beta_0 = 2.5$. The beginning of the constant displacement response range is at $T_D = 2.0$ s. The further required and used data are the design ground acceleration is $a_g = 0.168g$, the damping ratio is $\xi = 5\%$, the behavior factor is $q = 1.5$, the soil factor $S = 1.35$. Thus, the maximum spectral acceleration is $S_{\max} = 0.378g$. We remark that different types of choice would not affect the key findings about the effect of piecewise linearity. As our goal will be to discover the effect of the varying stiffness, scaling the spectrum (through any of the a_g, q or S parameters) would increase the support motion, the response, the response spectrum and the later defined piecewise linear spectrum at an equal rate. Thus, the rate of increment due to the piecewise-linearity would not be affected.

Fig. 1 (b) shows the $I(t)$ intensity function we used. The length of the strong motion period and the rate of the decay after that influences the response as it could allow the development of higher amplitude response terms near the resonance. We have chosen an intensity function characterizing an earthquake with a long strong motion period. In the first 2 seconds of the excitation, it has a quadratic increasing part. Between 2 s and 12 s, during the strong motion period, it equals 1. Finally, from 12 s to the end of the analyzed time (20 s), there is an exponentially decaying intensity ending at 0.0256 at $t = 20$ s.

For the $T_j = 2\pi/\omega_j$ periods of the harmonic components in Eq. (5) we first generated 40 periods between 0.1 s and 4 s, with an even distribution of their logarithm. First,

40 periods of harmonic components were generated with $T_j = e^{\ln(0.1)+(\ln(4)-\ln(0.1))(j-1)/39}$, and $j = 1\ldots40$. Dense distribution of the T_j values in the high period range caused often failure of the iteration process. To avoid this, for the accelerogram generation, we skipped the odd periods above the 1.5 s limit (i.e. the 31st, 33rd, … 39th).

To generate an accelerogram, we followed the iteration scheme recommended in [10]. After the random phase angles were chosen, the $\ddot{z}(t)$ function were generated with arbitrary initial A_j amplitudes. Then, the response spectrum of the $\ddot{z}(t)$ function was evaluated at the harmonics' frequencies. Then, the A_j amplitudes were modified linearly by the ratio of the target spectrum and the evaluated spectrum values and a new iteration step was initiated with a new $\ddot{z}(t)$ function. (Thus, the coupling between the frequencies were neglected in an iteration step.) We stopped the iteration, when all ratios reached 1 within a 0.1% error.

Fig. 2 (a) shows one example of the $\ddot{z}(t)$ acceleration functions, and Fig. 2 (b) shows the response spectrum of the same function. The fitting is obtained in the periods corresponding to the periods of the function. The blue line segments connect the fitted points. The error of those fitted values did not exceed 0.1% in the examples used.

We calculated the response spectrum for a 10 times finer mesh of periods, which is shown in the red line. (Those points were evaluated at a total of 391 periods with $T_k = e^{\ln(0.1)+(\ln(4)-\ln(0.1))(k-1)/390}$, and $k = 1...391$.) As we can observe, there is a difference between the target spectrum (shown in green for reference) and the actual spectrum. In the 20 examples we used in the analysis, the difference varied between 8% and 40%, with an average of 20%. This finer resolution is sufficiently dense to treat the result as a continuous line, and the neighboring maximum displacements occur at similar time instances in similar structures (with periods close to each other). Whenever there is a break in the segments, the time instant of the maximum changes radically. It means that a time-history analysis with an artificial function may have this difference with respect to the target spectrum from the excitation itself.

We mention here that higher number of harmonics in Eq. (5) could probably decrease these differences. However, it would increase the number of amplitudes which must be fitted, and due to the denser distribution of the harmonic frequencies, it could happen that the iteration would not converge.

2.3 Response of piecewise linear elastic structures

The simplest mechanical model is an SDOF system with two states: state *I* and *II*, with the natural circular frequencies of ω_I and ω_{II}, respectively, and the boundary between the states is at $u = 0$. See Fig. 3 for an example of this structure. There, a negative u displacement opens the gap at the k_{II} spring, leaving the k_I spring active, while a positive u displacement opens the gap at the k_I spring, leaving the k_{II} spring active. Thus in Eq. (2), the ω_0 will depend on the current state:

$$\omega_0 = \begin{cases} \omega_I = \sqrt{\dfrac{k_I}{m}}, & \text{if } u \le 0 \\ \omega_{II} = \sqrt{\dfrac{k_{II}}{m}}, & \text{if } 0 < u \end{cases} . \tag{6}$$

This model has a fully elastic impact without any energy loss caused by it. The free vibration of the model would be a piecewise harmonic vibration: in the state *I*, the half period would be the half of $T_I = 2\pi/\omega_I$, while in the state *II*, the half period would be the half of $T_{II} = 2\pi/\omega_{II}$, resulting in a $T_{PL} = (T_I + T_{II})/2$ period of the free vibration.

We apply the generated accelerograms as the support vibrations for the PL-elastic structures. The time-history analysis is performed using the Newmark method; the timestep is the same ($dt = 0.0005$ s) as what we used for the fitting. The response depends on two natural circular frequencies and their order, too. Let us denote the response of a system with $T_I = \alpha$ and $T_{II} = \beta$ by $u^{\alpha,\beta}(t)$.

In the case of a linear system, the opposite forcing ($-z(t)$) would result in the opposite response ($-u(t)$). The absolute value of the opposite response would be the same, and as such, the spectrum value would be the same. This is also the reason why there is no sign needed for the A_j amplitudes, as the possible opposite direction would be covered by the 2π range of the φ_j phase angles instead of the π range and the possible negative amplitude.

In the case of the PL-elastic system, the opposite forcing results in a different response, i.e., with the above notation of the response: $u^{\alpha,\beta}(t) \neq -u^{\beta,\alpha}(t)$. The sign of the actual response affects the further application, as well. A negative $u^{\alpha,\beta}(t)$ means that the structure is in the state *I*, so the direction of an equivalent static force should be chosen such that the static response occurs in that state. Similarly, a positive $u^{\alpha,\beta}(t)$ means that the structure is in the state *II*, so the direction of an equivalent static force should be chosen such that the static response occurs in that state.

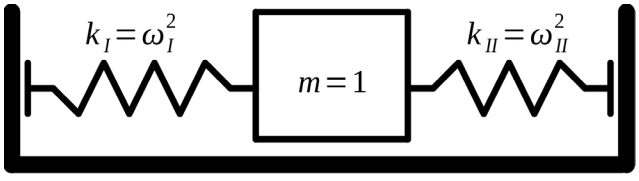

Fig. 3 Simple model of piecewise linear elastic structure of the analysis

3 Spectrum of PL-structures

For the piecewise-linear displacement spectrum, we have to distinguish between the state *I* and state *II*, according to Eq. (6). Instead of Eq. (3) with the absolute value, we have to specify the states separately, as

$$S_u^I\left(T_I,T_{II}\right)=-\min\left(u^{T_I,T_{II}}\left(t\right)\right),$$
$$S_u^{II}\left(T_I,T_{II}\right)=\max\left(u^{T_I,T_{II}}\left(t\right)\right). \tag{7}$$

As the vibration starts from $u(0) = 0$, the minimum response will be non-positive and corresponds to the state *I*, while the maximum is non-negative and corresponds to state *II*.

Similarly, the piecewise-linear pseudo-acceleration spectrum (the PL-spectrum) must be defined for each state, as

$$S_{PA}^I\left(T_I,T_{II}\right)=\omega_I^2 S_u^I\left(T_I,T_{II}\right),$$
$$S_{PA}^{II}\left(T_I,T_{II}\right)=\omega_{II}^2 S_u^{II}\left(T_I,T_{II}\right). \tag{8}$$

The diagrams of Fig. 4 (a) and (b) show these PL-spectra for both states, computed for the example accelerogram shown in Fig. 2 (a). The responses were evaluated on the 191 × 191 grid of T_I and T_{II} values in the logarithmic distribution between 0.1 s and 4 s. Thus, the T_j periods of the harmonic components are grid values of the calculation.

The diagrams of Fig. 4 (a) and (b) relate to Fig. 2 (b), as follows. The $T_I = T_{II}$ section of both diagrams corresponds to a linear system with the same stiffness in both states. These two curves can be projected above each other, and in each T_0 period, the higher value is the same as the spectrum of the current excitation (see Fig. 2 (b)).

We call the attention of the reader to two things. First, the surfaces have a wavy structure, which is caused by the different occurrence of the maximum values. Second, the unit of these diagrams is *g*, and there are enormous values appearing in each state's PL-spectrum when the period of the other state is small. The limit case of this latter phenomenon would be a spring with infinite stiffness on the affected side, which would be equivalent to an elastic impact with a rigid wall. At the same time, the compression of the spring with high relative stiffness (low period) would tend toward zero and the displacement response spectrum would go to zero. It can be seen on the displacement response spectrum diagrams of Fig. 5 (a) and (b).

4 Results

The $S_{PA}^I(T_I, T_{II})$ and $S_{PA}^{II}(T_I, T_{II})$ piecewise linear pseudo-acceleration spectra can be used for the evaluation of the extremal internal forces: in the state *I* the $-m \times S_{PA}^I(T_I, T_{II})$,

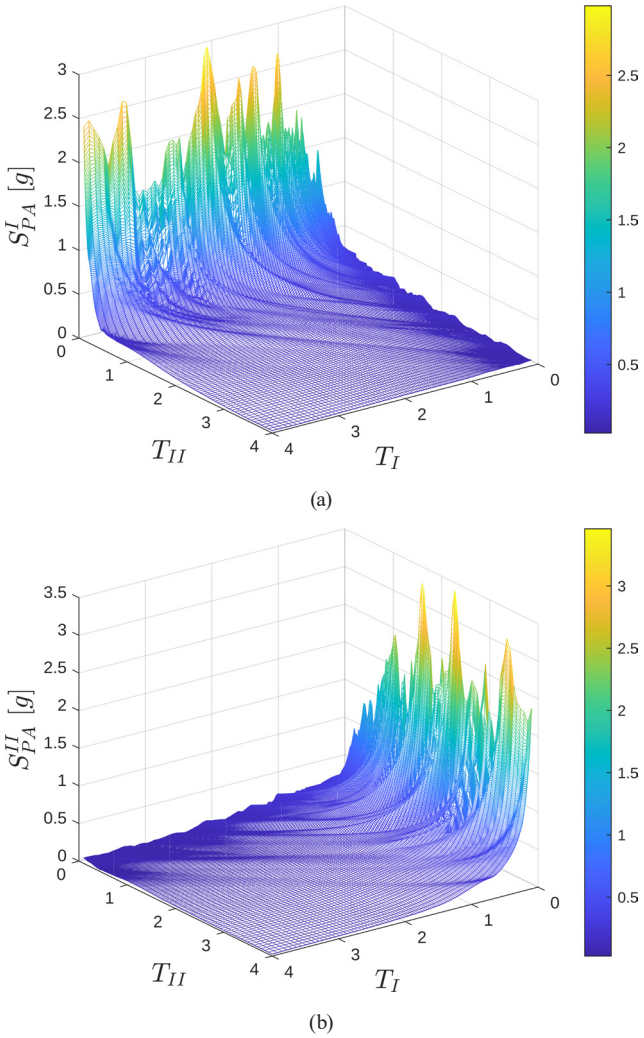

Fig. 4 Extremal values of the response of piecewise linear systems (a) The minimum pseudo accelerations in state *I*, (b) The maximum pseudo accelerations in state *II*

in state *II* the $m \times S_{PA}^{II}(T_I, T_{II})$ force yields the same extremal displacements as the actual support motion.

As we can see, there are extremely large maximum values, so it is important to analyze the relationship of the PL-spectrum to the spectrum of the linear system. In other words, what would happen if we omitted the PL-elasticity from the calculation?

The S_{PA}^I spectrum can be used in the state *I* only, so it is relevant if we take T_I as its principal variable. Looking at the diagram from the T_I-axis would show the $T_I < T_{II}$ and the $T_I > T_{II}$ cases combined, and due to the overlapping surfaces, we could not distinguish between the safe (where the maximum is not exceeding the linear spectrum value) and unsafe domains. So, to compare to the linear system, let us divide the S_{PA}^I-spectrum by the target spectrum value of the same linear system of state *I*:

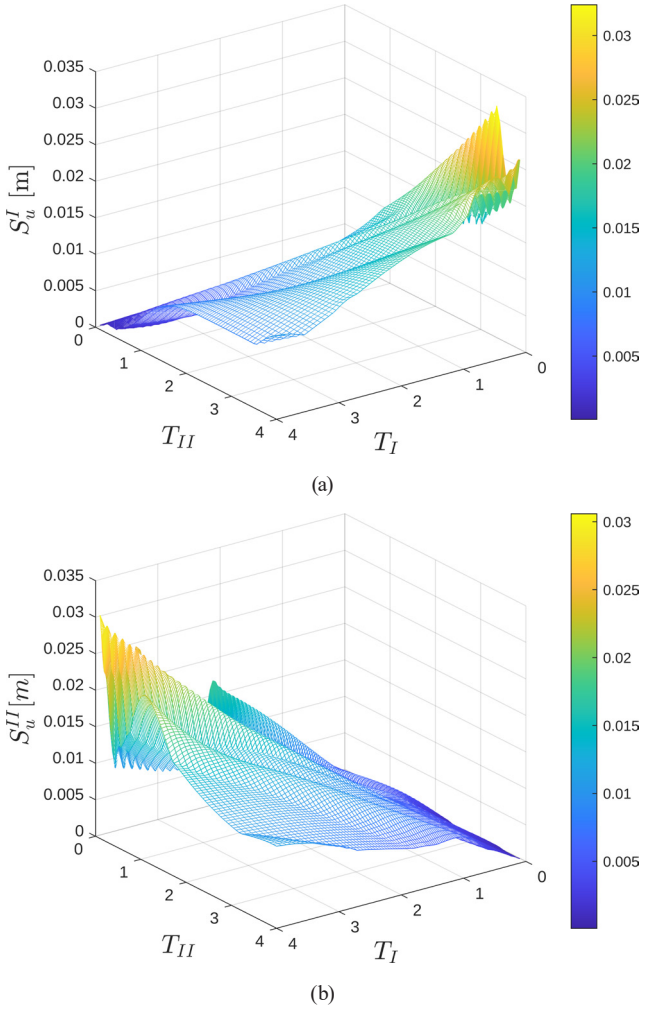

Fig. 5 Extremal values of the response of piecewise linear systems (a) The minimum displacements in state *I*, (b) The maximum displacements in state *II*

$$r_I\left(T_I,T_{II}\right)=\frac{S_{PA}^I\left(T_I,T_{II}\right)}{S_d\left(T_I\right)}. \tag{9}$$

Similarly, the S_{PA}^{II} spectrum can be used in the state *II* only, so it is relevant if we take T_{II} as its principal variable. To compare it to the linear system, let us divide the S_{PA}^{II}-spectrum by the target spectrum value of the same linear system of state *II*:

$$r_{II}\left(T_I,T_{II}\right)=\frac{S_{PA}^{II}\left(T_I,T_{II}\right)}{S_d\left(T_{II}\right)}. \tag{10}$$

In the r_I surface, the value below 1 means that the maximum displacement of the PL-system in state *I* is smaller than that of the linear system with the application of the target spectrum (i.e., the application of the design spectrum is on the safe side in this case). A value above 1 means that the maximum displacement of the PL-system in state *I* is higher than that of the linear system with the application of the target spectrum. The same can be said about the r_{II} surface. See the example surfaces in Fig. 6 (a) and (b) for states *I* and *II*, respectively.

As with the PL-spectra, in the r_I and r_{II} diagrams, there are domains where the values are much higher than 1. These highly unsafe domains occur where the period of the other state is much lower, i.e. that state is stiffer. In these cases, the elastic switch into the stiffer state results in a higher velocity at the switch backwards, as opposed to the linear case; thus, the amplitude of the response increases.

At the calculation of the spectrum of the generated accelerograms, we have seen that the actual maximum ratio of a spectrum to the design spectrum exceeds the 1 value (see Fig. 2 (b)). So, it is reasonable to accept as safe those domains of the *r*-surfaces, where the ratio does not exceed the maximum ratio of the linear spectrum. With that limit, we can define the safe and unsafe T_I-T_{II}-pairs for

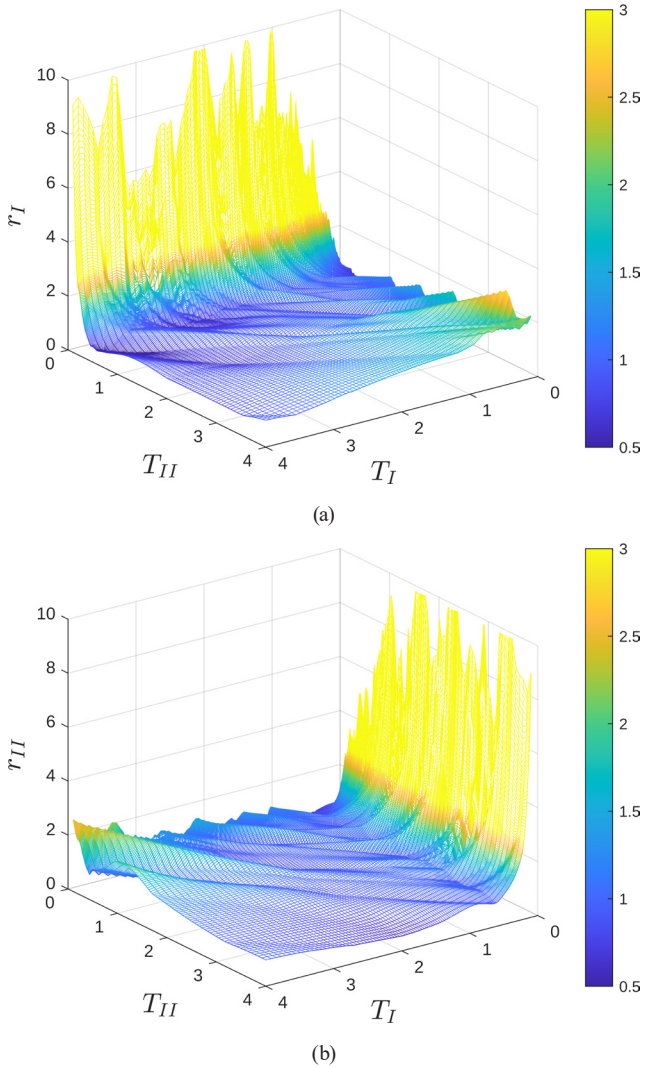

Fig. 6 Ratio of the PL-spectrum to the relevant linear spectrum in the example accelerogram function (a) in state *I*, (b) in state *II*

the given $\ddot{z}(t)$-accelerogram. In Fig. 7 (a) we demonstrate this on the accelerogram used in the previous examples (see Fig. 2 (a)): the white domains represent those T_I-T_{II} pairs, where both ratio of the PL-responses to the linear responses do not exceed the maximum ratio of the linear system, while in the blue domains one of the ratios are above the threshold. In the current example, this was a 14% difference. In the PL calculations, the direction of the excitation makes a difference in the response. That is the reason why the diagram is not symmetric.

If we consider the same excitation with both possible directions, then we have to combine this diagram with its mirrored version on the 1:1-line. There, only those points can be considered safe where both diagrams are in the safe domain. This modified diagram is shown in Fig. 7 (b). The upper and lower domains have a common point at $T_I = T_{II} \approx 1.1$, where the maximum ratio of the linear system occurred.

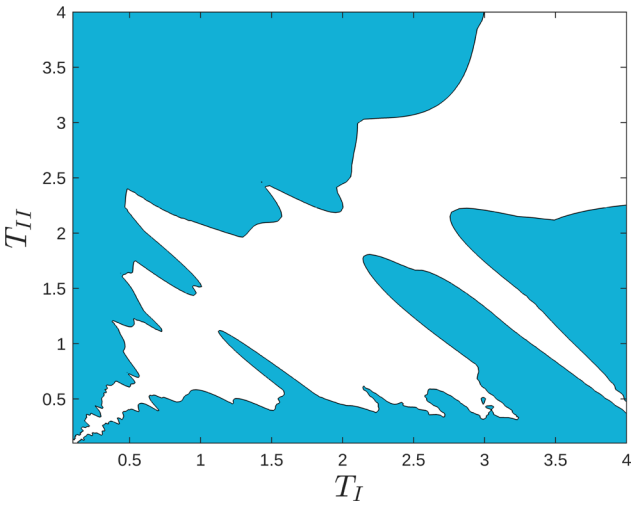

(a)

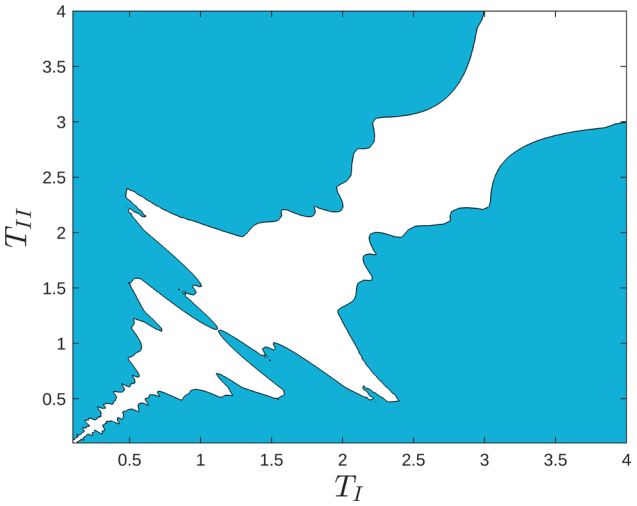

(b)

Fig. 7 Safe and unsafe domains of the PL-spectrum (a) in the sample excitation, (b) with the bidirectional excitation

For more general conclusions, we performed the same analysis for the 20 generated accelerograms. In each case, we identified the safe and unsafe domains of the T_I–T_{II}-plane on the 191 × 191-grid. For the summation, we calculated the number of unsafe cases in each grid-point. The results are shown in Fig. 8. In the darkest blue domain, the number of unsafe cases is zero. If the PL-elastic structure's two states have period-pairs in this domain, then the linear assessment does not have more error than the PL time history analysis.

In practical cases, the opening and closing of the cracks in a RC-structure causes just a small change in the global stiffness, and thus in the period. Because of that, the stiffnesses and the periods are close to each other. In Fig. 8, we marked two white lines, where the ratio of the two periods differs from 1 by 6% only (these lines align with the grid of the evaluated period values due to the exponential distribution). We can see that between these two lines, the domain is safe in most cases. In Fig. 9, we show the number of time histories (out of the 20 examples) where the maximum ratio is higher than the maximum ratio of the linear system. Out of the 188 grid points, only 6 has more than 1 case where the PL-spectrum would exceed the linear spectrum. There is a single peak value around the $T \approx 2.5$ value, where up to five cases (out of 20) could become unsafe.

5 Conclusions

We have shown a generalization of the concept of spectrum for PL-elastic structures. We found that for single DOF systems, there is no significant effect from the nonlinearity on the response as long as the difference in stiffness is not significant. Our findings also give a reassuring justification of the application of the linear response spectrum for structures with this low level of nonlinearity.

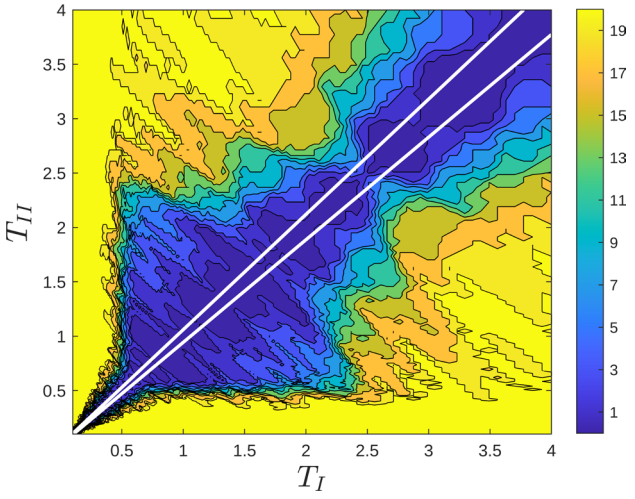

Fig. 8 Combined diagram of the 20 PL-spectra ratios: number of unsafe PL-cases out of 20, with the white lines of the 6% threshold of the periods

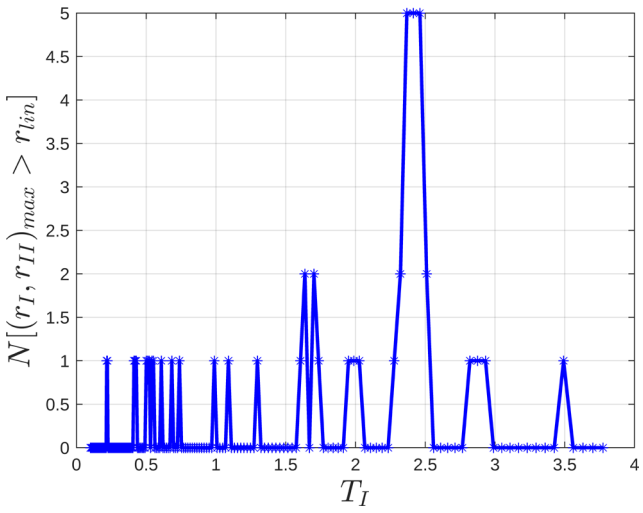

Fig. 9 Number of unsafe PL-cases out of 20, along the upper white line of Fig. 8

As the repeated opening and closing of the crack in a reinforced concrete structure modifies the stiffness and thus, the period of the structure, the neglect of this nonlinearity does not introduce more difference in the assessment than the time-history analysis could generate.

We expect that the switch at a different configuration than the equilibrium position (e.g. due to a prestressing force, or an open crack in the equilibrium position) will affect our findings on the safe side. The maximum velocities occur near the equilibrium position, so the velocity at the switch will be lower. Thus, the amplification caused by the switch backwards will have a lower effect.

Our analysis was restricted to the SDOF systems. In multi-degree-of-freedom systems, the modal analysis would involve the switch between the linear vibration modes at the time of switching. By this switch, the energy of each mode is distributed among the other modes. Thus, we expect that the high values of Fig. 4 (a) and (b) will be damped. So, the large differences in the order of magnitudes of different vibration frequencies would not play a significant role in that case either.

Acknowledgement
The project presented in this article is supported by OTKA project K138615.

References

[1] CEN "CEN EN 1998-1:2004 Eurocode 8: Design of Structures for Earthquake Resistance – Part 1: General rules, seismic actions and rules for buildings", European Committee for Standardization, Brussels, Belgium, 2004.

[2] National Institute of Building Sciences "Earthquake-Resistant Design Concepts: An Introduction to the NEHRP Recommended Seismic Provisions for New Buildings and Other Structures", Federal Emergency Management Agency of the U. S. Department of Homeland Security, Hyattsville, MD, USA, FEMA P-749, 2010.

[3] Takeda, T., Sozen, M. A., Nielsen, N. N. "Reinforced Concrete Response to Simulated Earthquakes", Journal of the Structural Division, 96(12) pp. 2557–2573, 1970. https://doi.org/10.1061/JSDEAG.0002765

[4] Nodeh Farahani, R., Abdollahzadeh, G., Mirza Goltabar Roshan, A. "The Modified Energy-based Method for Seismic Evaluation of Structural Systems with Different Hardening Ratios and Deterioration Hysteresis Models", Periodica Polytechnica Civil Engineering, 68(1), pp. 37–56, 2024. https://doi.org/10.3311/PPci.21359

[5] Ayengin, Ş., Bağbancı, M. B., Köprülü Bağbancı, Ö. "Evaluation of Material Characteristics and Structural Dynamic Properties of a Historical Church: The Case of 19th Century Bursa Derekoy Church (Ayia Paraskevi)", Periodica Polytechnica Civil Engineering, 68(3), pp. 797–811, 2024. https://doi.org/10.3311/PPci.22520

[6] Bianchini, N., Mendes, N., Lourenço, P. B., Calderini, C. "Modelling of the Dynamic Response of a Full-Scale Masonry Groin Vault: Unstrengthened and Strengthened with Textile-Reinforced Mortar (TRM)", International Journal of Architectural Heritage, 18(12), pp. 2042–2066, 2024. https://doi.org/10.1080/15583058.2024.2320857

[7] Németh, R. K., Geleji, B. B. "Nonlinear Normal Modes of a Piecewise Linear Continuous Structure with a Regular State", Periodica Polytechnica Civil Engineering, 62(4), pp. 1039–1051, 2018. https://doi.org/10.3311/PPci.12512

[8] Várkonyi, P. L., Kocsis, M., Ther, T. "Rigid impacts of three-dimensional rocking structures", Nonlinear Dynamics, 107(3), pp. 1839–1858, 2022. https://doi.org/10.1007/s11071-021-06934-x

[9] Ruggieri, S., Uva, G. "Extending the concepts of response spectrum analysis to nonlinear static analysis: Does it make sense?", Innovative Infrastructure Solutions, 9(7), 235, 2024. https://doi.org/10.1007/s41062-024-01561-y

[10] Gasparini, D. A., Vanmarcke, E. "Simulated Earthquake Motions Compatible with Prescribed Response Spectra, Evaluation of seismic safety of buildings", Department of Civil Engineering, Massachusetts Institute of Technology, Cambridge, MA, USA, Rep. R76-4, 1976.

[11] Colajanni, P., Pagnotta, S., Testa, G. "Comparison of fully non-stationary artificial accelerogram generation methods in reproducing seismicity at a given site", Soil Dynamics and Earthquake Engineering, 133, 106135, 2020. https://doi.org/10.1016/j.soildyn.2020.106135